Observing Application

Date:	Jun 22, 2020
Proposal ID:	GBT/20A-572
Legacy ID:	QB297
PI:	Michael Busch
Type:	Director's Discretionary Time - Exploratory Time
Category:	Interstellar Medium
Total time:	81.7

A GBT Search for High Latitude "CO-Dark" Molecular Gas

Abstract:

This proposal is in response to the call for low-frequency GBT proposals during the Infectious Disease Operating Status (IDOS) initiated on March 16th. We propose to use a CO high latitude survey (Heithausen et al. 1993) as a guide for a search for high latitude dark molecular gas, which is observed to be widespread in the disk of the Galaxy. Donate 2019 discovered three times more mass traced by OH than CO in the high latitude cloud MBM 53, however no sightlines without CO emission were detected. There are 29 positions in Heithausen et al. of maximum CO intensity that we can trace with OH and compare the resulting molecular mass traced. Additionally, there are 9 pointings where CO emission was expected from an excess of IR emission, but no CO emission or weak emission were found. These are excellent candidate sight lines for OH emission because OH has been shown to trace diffuse molecular gas which CO is not collisionally excited in (e.g. Busch 2019). These results will shed light on how extended the dark gas is from canonical CO clouds at high latitudes, and how much more dark baryons there might be in the Galactic Halo.

Authors:

Name	Institution	Email	Status
Busch, Michael	Johns Hopkins University	mpbusch@jhu.edu	Graduating: 2016 Thesis: true
Allen, Ron	Space Telescope Science Institute	rjallen@stsci.edu	

Principal Investigator:	Michael Busch
Contact:	Michael Busch
Telephone:	520-280-7151
Email:	mpbusch@jhu.edu

Related Proposals:

Joint:

Not a Joint Proposal.

Observing type(s):

Spectroscopy, Grid Mapping/Mosaicing

GBT Resources

Name	Group	Frontend & Backend	Setup
Galpos	GalPos1	L-Band (1.15-1.73 GHz) VEGAS	Observing type: Spectral Line Number of beams: 1 Number of spectrometers: 8

Spectrometer #	1	2	3	4	5	6	7	8
Mode	15	15	15	15	15	15	15	15
Bandwidth (MHz)	11.72	11.72	11.72	11.72	11.72	11.72	11.72	11.72
Rest frequences (GHz)	1.617	1.666	1.720	1.17651	1.45143	1.47807	1.56198	1.59135
Spectral resolution (KHz)	0.4	0.4	0.4	0.4	0.4	0.4	0.4	0.4
Integration time (s)	5.0	5.0	5.0	5.0	5.0	5.0	5.0	5.0
Data rate (MB/s)	0.1	0.1	0.1	0.1	0.1	0.1	0.1	0.1

Sources

Name	Position		Velocity		Group
119070+2800	Coordinate system	Equatorial	Convention	Radio	HighCO
	Equinox	J2000			
	Right Ascension	17:50:44.50	Ref. frame	LSRK	
		00:00:00			
	Declination	+86:28:04.00	Velocity	0	
		00:00:00			
	Calibrator	No			
119210+2000	Coordinate system	Equatorial	Convention	Radio	HighCO
	Equinox	J2000			
	Right Ascension	23:06:03.80	Ref. frame	LSRK	
		00:00:00			
	Declination	+82:06:34.00	Velocity	0	
		00:00:00			
	Calibrator	No			
120500+2963	Coordinate system	Equatorial	Convention	Radio	HighCO
	Equinox	J2000			
	Right Ascension	15:32:18.50	Ref. frame	LSRK	
		00:00:00			
	Declination	+86:42:50.00	Velocity	0	
		00:00:00			
	Calibrator	No			

Name	Position		Velocity		Group
120500+1863	Coordinate system	Equatorial	Convention	Radio	HighCO
	Equinox	J2000			
	Right Ascension	23:50:24.00	Ref. frame	LSRK	
		00:00:00			
	Declination	+81:13:13.00	Velocity	0	
		00:00:00			
	Calibrator	No			
121070+2175	Coordinate system	Equatorial	Convention	Radio	HighCO
	Equinox	J2000			
	Right Ascension	23:39:53.50	Ref. frame	LSRK	
		00:00:00			
	Declination	+84:22:08.00	Velocity	0	
		00:00:00			
	Calibrator	No			
121930+1975	Coordinate system	Equatorial	Convention	Radio	HighCO
	Equinox	J2000			
	Right Ascension	00:22:12.70	Ref. frame	LSRK	
		00:00:00			
	Declination	+82:34:29.00	Velocity	0	
		00:00:00			
	Calibrator	No			
122220+1875	Coordinate system	Equatorial	Convention	Radio	HighCO
	Equinox	J2000			
	Right Ascension	00:32:58.10	Ref. frame	LSRK	
		00:00:00			
	Declination	+81:36:17.00	Velocity	0	
		00:00:00			
	Calibrator	No			
122500+2900	Coordinate system	Equatorial	Convention	Radio	HighCO
	Equinox	J2000			
	Right Ascension	13:37:04.30	Ref. frame	LSRK	
		00:00:00			
	Declination	+88:05:39.00	Velocity	0	
		00:00:00			
	Calibrator	No			
123500+1963	Coordinate system	Equatorial	Convention	Radio	HighCO
	Equinox	J2000			
	Right Ascension	01:07:48.80	Ref. frame	LSRK	
		00:00:00			
	Declination	+82:29:02.00	Velocity	0	
		00:00:00			
	Calibrator	No			

Name	Position		Velocity		Group
123360+2075	Coordinate system	Equatorial	Convention	Radio	HighCO
	Equinox	J2000			
	Right Ascension	01:05:50.00	Ref. frame	LSRK	
		00:00:00			
	Declination	+83:36:59.00	Velocity	0	
		00:00:00			
	Calibrator	No			
125070+1950	Coordinate system	Equatorial	Convention	Radio	HighCO
	Equinox	J2000			
	Right Ascension	01:50:55.20	Ref. frame	LSRK	
		00:00:00			
	Declination	+82:07:42.00	Velocity	0	
		00:00:00			
	Calibrator	No			
125220+3250	Coordinate system	Equatorial	Convention	Radio	HighCO
	Equinox	J2000			
	Right Ascension	11:32:32.90	Ref. frame	LSRK	
		00:00:00			
	Declination	+84:16:42.00	Velocity	0	
		00:00:00			
	Calibrator	No			
125500+2200	Coordinate system	Equatorial	Convention	Radio	HighCO
	Equinox	J2000			
	Right Ascension	02:31:34.00	Ref. frame	LSRK	
		00:00:00			
	Declination	+84:22:33.00	Velocity	0	
		00:00:00			
	Calibrator	No			
126500+3250	Coordinate system	Equatorial	Convention	Radio	HighCO
	Equinox	J2000			
	Right Ascension	10:55:06.00	Ref. frame	LSRK	
		00:00:00			
	Declination	+83:48:07.00	Velocity	0	
		00:00:00			
	Calibrator	No			
127500+2088	Coordinate system	Equatorial	Convention	Radio	HighCO
	Equinox	J2000			
	Right Ascension	03:10:13.30	Ref. frame	LSRK	
		00:00:00			
	Declination	+82:29:30.00	Velocity	0	
		00:00:00			
	Calibrator	No			

Name	Position		Velocity		Group
142210+2325	Coordinate system	Equatorial	Convention	Radio	HighCO
	Equinox	J2000			
	Right Ascension	06:18:19.10	Ref. frame	LSRK	
		00:00:00			
	Declination	+72:09:36.00	Velocity	0	
		00:00:00			
	Calibrator	No			
143000+3850	Coordinate system	Equatorial	Convention	Radio	HighCO
	Equinox	J2000			
	Right Ascension	09:28:08.80	Ref. frame	LSRK	
		00:00:00			
	Declination	+69:44:30.00	Velocity	0	
		00:00:00			
	Calibrator	No			
143360+2425	Coordinate system	Equatorial	Convention	Radio	HighCO
	Equinox	J2000			
	Right Ascension	06:34:08.30	Ref. frame	LSRK	
		00:00:00			
	Declination	+71:23:34.00	Velocity	0	
		00:00:00			
	Calibrator	No			
146070+1775	Coordinate system	Equatorial	Convention	Radio	HighCO
	Equinox	J2000			
	Right Ascension	05:35:54.00	Ref. frame	LSRK	
		00:00:00			
	Declination	+66:42:05.00	Velocity	0	
		00:00:00			
	Calibrator	No			
146200+3963	Coordinate system	Equatorial	Convention	Radio	HighCO
	Equinox	J2000			
	Right Ascension	09:26:49.60	Ref. frame	LSRK	
		00:00:00			
	Declination	+67:00:30.00	Velocity	0	
		00:00:00			
	Calibrator	No			
146930+2075	Coordinate system	Equatorial	Convention	Radio	HighCO
	Equinox	J2000			
	Right Ascension	06:07:15.70	Ref. frame	LSRK	
		00:00:00			
	Declination	+67:12:05.00	Velocity	0	
		00:00:00			
	Calibrator	No			

Name	Position		Velocity		Group
147000+4038	Coordinate system	Equatorial	Convention	Radio	HighCO
	Equinox	J2000			
	Right Ascension	09:30:54.70	Ref. frame	LSRK	
		00:00:00			
	Declination	+66:07:51.00	Velocity	0	
		00:00:00			
	Calibrator	No			
147200+4075	Coordinate system	Equatorial	Convention	Radio	HighCO
	Equinox	J2000			
	Right Ascension	09:33:29.00	Ref. frame	LSRK	
		00:00:00			
	Declination	+65:49:44.00	Velocity	0	
		00:00:00			
	Calibrator	No			
148200+3863	Coordinate system	Equatorial	Convention	Radio	HighCO
	Equinox	J2000			
	Right Ascension	09:11:26.00	Ref. frame	LSRK	
		00:00:00			
	Declination	+65:59:15.00	Velocity	0	
		00:00:00			
	Calibrator	No			
148210+2350	Coordinate system	Equatorial	Convention	Radio	HighCO
	Equinox	J2000			
	Right Ascension	06:37:51.10	Ref. frame	LSRK	
		00:00:00			
	Declination	+66:54:20.00	Velocity	0	
		00:00:00			
	Calibrator	No			
151500+1925	Coordinate system	Equatorial	Convention	Radio	HighCO
	Equinox	J2000			
	Right Ascension	06:04:14.40	Ref. frame	LSRK	
		00:00:00			
	Declination	+62:39:35.00	Velocity	0	
		00:00:00			
	Calibrator	No			
153640+1925	Coordinate system	Equatorial	Convention	Radio	HighCO
	Equinox	J2000			
	Right Ascension	06:15:16.60	Ref. frame	LSRK	
		00:00:00			
	Declination	+60:47:15.00	Velocity	0	
		00:00:00			
	Calibrator	No			

Name	Position		Velocity		Group
156540+3513	Coordinate system	Equatorial	Convention	Radio	HighCO
	Equinox	J2000			
	Right Ascension	08:27:26.10	Ref. frame	LSRK	
		00:00:00			
	Declination	+60:18:14.00	Velocity	0	
		00:00:00			
	Calibrator	No			
156640+3250	Coordinate system	Equatorial	Convention	Radio	HighCO
	Equinox	J2000			
	Right Ascension	08:01:55.40	Ref. frame	LSRK	
		00:00:00			
	Declination	+60:32:04.00	Velocity	0	
		00:00:00			
	Calibrator	No			
119380+3967	Coordinate system	Equatorial	Convention	Radio	LowCO
	Equinox	J2000			
	Right Ascension	13:40:49.90	Ref. frame	LSRK	
		00:00:00			
	Declination	+77:07:34.0	Velocity	0	
		00:00:00			
	Calibrator	No			
122290+4133	Coordinate system	Equatorial	Convention	Radio	LowCO
	Equinox	J2000			
	Right Ascension	12:59:17.60	Ref. frame	LSRK	
		00:00:00			
	Declination	+75:47:31.0	Velocity	0	
		00:00:00			
	Calibrator	No			
131430+4667	Coordinate system	Equatorial	Convention	Radio	LowCO
	Equinox	J2000			
	Right Ascension	11:44:37.50	Ref. frame	LSRK	
		00:00:00			
	Declination	+69:20:42.0	Velocity	0	
		00:00:00			
	Calibrator	No			
132220+3167	Coordinate system	Equatorial	Convention	Radio	LowCO
	Equinox	J2000			
	Right Ascension	08:57:33.30	Ref. frame	LSRK	
		00:00:00			
	Declination	+80:43:56.0	Velocity	0	
		00:00:00			
	Calibrator	No			

Name	Position		Velocity		Group
134570+3400	Coordinate system	Equatorial	Convention	Radio	LowCO
	Equinox	J2000			
	Right Ascension	09:30:39.10	Ref. frame	LSRK	
		00:00:00			
	Declination	+77:52:18.0	Velocity	0	
		00:00:00			
	Calibrator	No			
137160+4300	Coordinate system	Equatorial	Convention	Radio	LowCO
	Equinox	J2000			
	Right Ascension	10:42:00.50	Ref. frame	LSRK	
		00:00:00			
	Declination	+70:22:49.0	Velocity	0	
		00:00:00			
	Calibrator	No			
150120+4067	Coordinate system	Equatorial	Convention	Radio	LowCO
	Equinox	J2000			
	Right Ascension	09:24:05.80	Ref. frame	LSRK	
		00:00:00			
	Declination	+63:51:19.0	Velocity	0	
		00:00:00			
	Calibrator	No			
155670+2133	Coordinate system	Equatorial	Convention	Radio	LowCO
	Equinox	J2000			
	Right Ascension	06:36:11.70	Ref. frame	LSRK	
		00:00:00			
	Declination	+59:41:03.0	Velocity	0	
		00:00:00			
	Calibrator	No			
157350+2200	Coordinate system	Equatorial	Convention	Radio	LowCO
	Equinox	J2000			
	Right Ascension	06:44:43.10	Ref. frame	LSRK	
		00:00:00			
	Declination	+58:23:15.0	Velocity	0	
		00:00:00			
	Calibrator	No			

Sessions:

Name	Session time (hours)	Repeat	Separation	LST minimum	LST maximum	Elevation minimum
1	2.15	29	0 day	00:00:00	23:59:60	15
2	2.15	9	0 day	00:00:00	23:59:60	15

Session Constraints:

Name	Scheduling constraints	Comments
1	No constraints	
2	No constraints	

Session Source/Resource Pairs:

Session name	Source	Resource	Time
1	119070+2800 119210+2000 120500+2963 120500+1863 121070+2175 121930+1975 122220+1875 122500+2900 123500+1963 123360+2075 125070+1950 125220+3250 125500+2200 126500+3250 127500+2088 142210+2325 143000+3850 143360+2425 146070+1775 146200+3963 146930+2075 147000+4038 147200+4075 148200+3863 148210+2350 151500+1925 153640+1925 156540+3513 156640+3250	Galpos	2.15 hour
2	119380+3967 122290+4133 131430+4667 132220+3167 134570+3400 137160+4300 150120+4067 155670+2133 157350+2200	Galpos	2.15 hour

Present for observation: no Staff support: Plan of dissertation: yes

Technical Justification:

Dates:

Null

Observing time:

The time estimate per pixel is based on the experience gained in AGBT13B_044 and AGBT14B_031.

There we used both polarizations, an observing channel width of 1.526 kHz, and the frequency-switched mode. Each pixel was observed for 12 scans of duration 10 minutes, which required about 11 minutes of clock time, since we balanced before each scan. the resultant rms after smoothing to 1 km/s was 3 mK, a value which we propose to reach in this session.

Mapping:

N/A

RFI considerations:

The potential impact of interference is discussed in the Science Justification.

Overhead:

Each session will begin with a pointing observation followed by slewing to the target source. The time required to move to the pointing source depends upon where the telescope was left. Once on the pointing source the process takes approximately 5 minutes. Each pixel requires approximately 128 minutes of observing time.

Joint considerations:

N/A

Novel considerations:

N/A

Pulsar considerations:

N/A

LST Range Justification:

N/A

Draft version June 22, 2020
Typeset using LaTeX default style in AASTeX63

A GBT Search for High Latitude Dark Molecular Gas
(DRAFT of a GBT proposal; June 22, 2020.)

Michael Busch (JHU) and Ron Allen (STScI)

1. BACKGROUND

Since 2012 our group at JHU has been studying extremely faint ($\overline{T}_{mb} < 0.1$K, see Fig. 1), thermal (non-maser) hydroxyl (OH) emission in the Outer Galaxy using the Green Bank Telescope (GBT). This emission is partly tied to a unique phase of the diffuse molecular interstellar medium (ISM) that is invisible to the conventional molecular gas tracer of the 3mm carbon monoxide (CO) line (e.g., Grenier et al. 2005; Wolfire et al. 2010). The spontaneous emission rate coefficients of OH is lower than CO by 10^3, and low enough that collisions with H_2 in extremely diffuse gas ($n \sim 1$ cm^{-3}) is sufficient for the ground state OH energy levels to radiative efficiently. Conversely, in diffuse gas, there is not enough collisions to sufficiently populate the CO J=1 state for the CO to remain bright. In two papers, Allen et al. (2015) and Busch et al. (2019) demonstrated that on large ($\Delta b, \Delta l = 1°$) and small ($\Delta b, \Delta l = 0.125°$) spatial scales, OH is observable in 50 and 80% more sightlines than CO in their respective survey areas. Busch et al. (2019) showed using diffuse cloud models from Neufeld & Wolfire (2016) that the OH-bright, CO-dark sightlines have characteristic volume densities lower than $n = 150$ cm^{-3}, while the OH-bright, CO-bright sightlines have volume densities greater than $n = 300$ cm^{-3}, consistent with a collisional excitation explanation of the dark gas. Recent simulations have come to similar conclusions (Seifried et al. 2019).

Dark gas has now been found to be abundant in the Galactic Plane through our GBT OH studies and other studies using neutral medium tracers like [CII] (Velusamy et al. 2010; Pineda et al. 2013; Glover & Smith 2016). Above the plane, the molecular content of the high-velocity cloud–and their mass–has remained an enduring mystery. Indirect molecular tracers such as excess IR emission from dust (Planck Collaboration et al. 2011) or excess gamma ray emission from interactions of cosmic rays with invisible material (Grenier et al. 2005; Abdo et al. 2010) have detected **diffuse excess material at high latitudes off of the galactic disk, but whether or not this material is, in fact, molecular is still under question.**

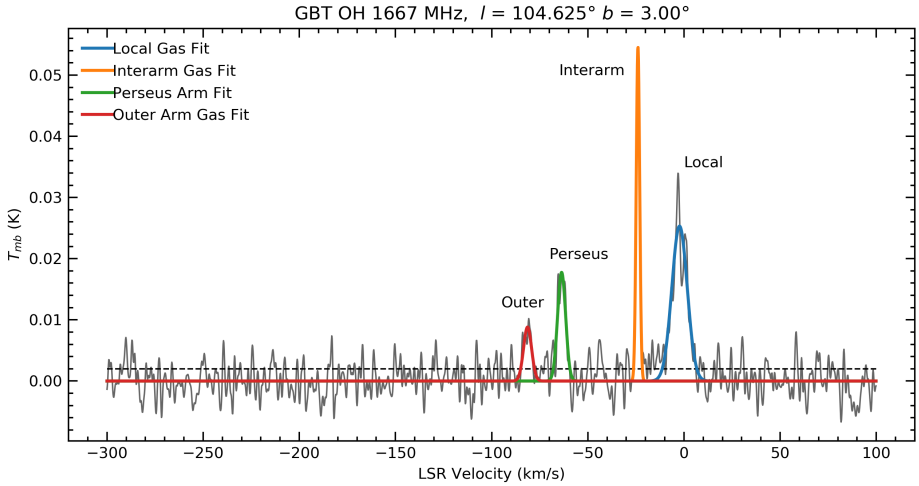

Figure 1. An example typical 2 hour GBT OH VEGAS spectrum towards the Outer Galaxy. Using the velocity structure of the Galaxy we are able to separate features into their components roughly based on distance. The spectrum has been smoothed to 1 km/s, and has a rms of about 2 mK. This is the type of spectrum we wish to produce from this proposal for high latitude sightlines. The high latitude gas has been seen in CO at local velocities (~ 0 km/s).

.

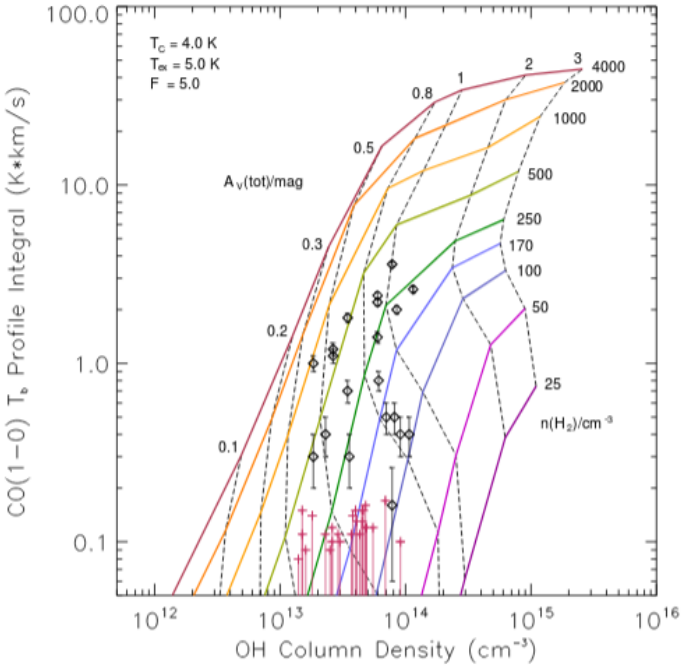

Figure 2. The column and volume density predictions of the 'One Square Degree' (figure from Busch et al. (2019)) using CO and OH observations in tandem to predict valuable gas properties using the diffuse cloud models of Neufeld & Wolfire (2016, 2017). The red points are the OH bright, CO dark sightlines which have only upper limits on the CO. We can combine the same information of the high latitude clouds and infer the physical environment of the gas.

In this program, we propose to leverage the excellent sensitivity of the GBT to tackle the long-standing question of the physical conditions and mass of the high-latitude clouds. **We will observe the Polaris Flare, Ursa Major and Camelopardalis high latitude clouds**, which have been mapped in CO (Heithausen et al. 1993). **We will obtain deep spectroscopy of the hyper-fine, lambda-doubling OH ground state lines at 1612, 1665, 1667 and 1720 MHz and 5 carbon radio recombination lines (CRRLs).** We will then supplement these observations with data for HI 21-cm from the LAB survey (Kalberla et al. 2005) and the CO J=1-0 observations from Heithausen et al. (1993), available in the literature. With these data, we will address the following long-standing questions: **is the dark gas at high latitudes molecular material? How do the OH and CO traced H_2 mass compare in these clouds? And what are the probable physical conditions of this gas?**

2. SCIENTIFIC MOTIVATION

As CO has been shown to be an unreliable tracer of diffuse molecular gas in the disk, we propose to look for "CO-Dark" molecular gas in the high latitude molecular clouds using GBT observations of the OH molecule. Spectroscopy of OH has proven to be a great tracer of molecular gas, and as it is an optically thin line, it also gives reliable mass estimates.

2.1. *Dark Baryons in the Galactic Halo?*

The first objective of this proposal is to directly observe the dark molecular gas using OH as a tracer. As dust and gas optical depth are highly correlated, Blitz et al. (1990) suggested that excess IR emission is a good tracer of molecular material that is not traced by CO. Whether or not this conclusion is correct is still up for debate. The excess material may be be atomic, rather than molecular gas, and is hidden in the form of optically thick HI, which underestimates atomic gas mass (Fukui et al. 2015). This may be expected as the HI brightness temperature approaches the gas temperature at around 90-100K. However, a recent study has shown using a new HI all-sky survey (GALFA-HI, Murray et al. (2018)) that the dark gas alone cannot be accounted for by optically thick HI. Undoubtedly, some of the excess IR material that is labeled dark gas may be optically thick HI, but some of it may also be diffuse molecular gas. **Our observations will be able to distinguish the dark gas between the two populations.**

The authors of the CO survey in Heithausen et al. (1993) suggested that since CO is seen at some of the sightlines with excess IR emission, but not all of them, that CO is the better tracer of molecular material than IR emission. We have shown however that CO is not a good tracer of the diffuse molecular gas in the aforementioned papers using sensitive OH observations with the GBT (Allen et al. 2015; Busch et al. 2019). **There be a large amount of diffuse molecular gas in these high latitude clouds that have never been observed, and contribute a large portion to the overall molecular mass content in the high latitude clouds in the Galactic Halo**. A detection of OH in a sightline without CO will unambiguously demonstrate the existence of the dark molecular gas in the high latitude cloud population.

2.2. *A Comparison of Tracers: The Physical Environment of the High Latitude Gas*

Another objective of this proposal is to **compare the mass traced by OH and CO in the same sightlines**. If one considers a static illuminated slab model of a photodissociation region, we would expect OH to form before CO as it is a hydride (Wolfire et al. 2010). A sufficient amount of H_2 column needs to form in order to shield the CO from the interstellar radiation field. As this column builds up, the O reservoir chemically moves from OH into CO at $A_v > 2$. Donate et al. (2019) recently observed OH towards the high latitude molecular clouds MBM 53 and compared the content traced by CO and OH. In their paper, they find that OH traces three times more molecular gas than CO. We propose that the OH is in fact tracing a larger volume of molecular gas along the line of sight than CO. We can check this conclusion by observing the high latitude clouds described in this proposal.

A major advantage of observing two molecular tracers in the same sightline is that we can perform modeling of the line strengths as we did in Busch et al. (2019) to deduce important properties of the gas itself such as **column densities, volume densities and gas temperature** (see Fig. 2). Not much is known about the high latitude clouds and this information can be essential in shedding light of the environment of this type of gas.

2.3. *Carbon Radio Recombination Lines: Fully Sampling the Gas Phase Structure of the High Latitude Gas*

We plan to use the same configuration as the approved project 20B-044, which includes simultaneously observing several Carbon Radio Recombination Lines (CRRL) in the L-band, which have been shown to trace a phase of the ISM where the carbon is primarily in C^+/C rather than CO (Salas et al. 2019). We are not aware of any CRRL observations towards high latitude gas, but the combination of CO (archival, Heithausen et al. (1993)), OH (this program), C^+ (this program), and HI (archival, Kalberla et al. (2005)) will fully sample the entire phase structure of the high latitude gas: from fully atomic, to semi-atomic, to molecular along the line of sight. CRRLs have been suggested to be good tracers of the dark gas for some time, but whether the CRRLs are co-spatial with OH emission (a known tracer of dark molecular gas) has yet to be seen.

3. PROPOSED OBSERVATIONS

The present request is a filler time proposal for 76 hours (+ overhead) to study the nature of dark (or diffuse) molecular gas in the high latitude molecular clouds using the GBT. There are 32 sightlines, for 2 hours a sightline, plus 10% for overhead.

The primary objective of this proposal is to observe OH in sightlines where CO was not present. We propose to observe the sightlines listed in Table 3 of Heithausen et al. (1993) for a direct comparison with the CO observations to accomplish this. There should be a strong corresponding OH signal, which we can then translate into a data point on a model grid like Fig. 2. **There are 9 sightlines where CO was not detected but excess IR emission was detected. These pointings are the ideal candidates to detect the dark molecular gas in OH.** These pointings are in red in Fig. 3.

A secondary objective of this proposal is to compare directly the mass traced by both CO and OH by observing the positions listed in Table 1 of Heithausen et al. (1993). These positions are the most intense CO brightness temperatures detected in individual clouds. Since we cannot fully sample the clouds in OH using the GBT without an unusually large amount of time, we will have to assume an average molecular mass multiplied by the area listed in Table 1 and compare those numbers with the mass traced by CO. Additionally, we can derive many important gas properties using the diffuse cloud models as used in Busch et al. (2019). These pointings are in white in Fig. 3.

4. RADIO FREQUENCY INTERFERENCE (RFI)

Recent observing runs have provided first-hand experience with several sources of 18-cm RFI at the GBT. The 18-cm interference is not too intense and is far enough from the OH lines to be easily masked, so a single IF can include both

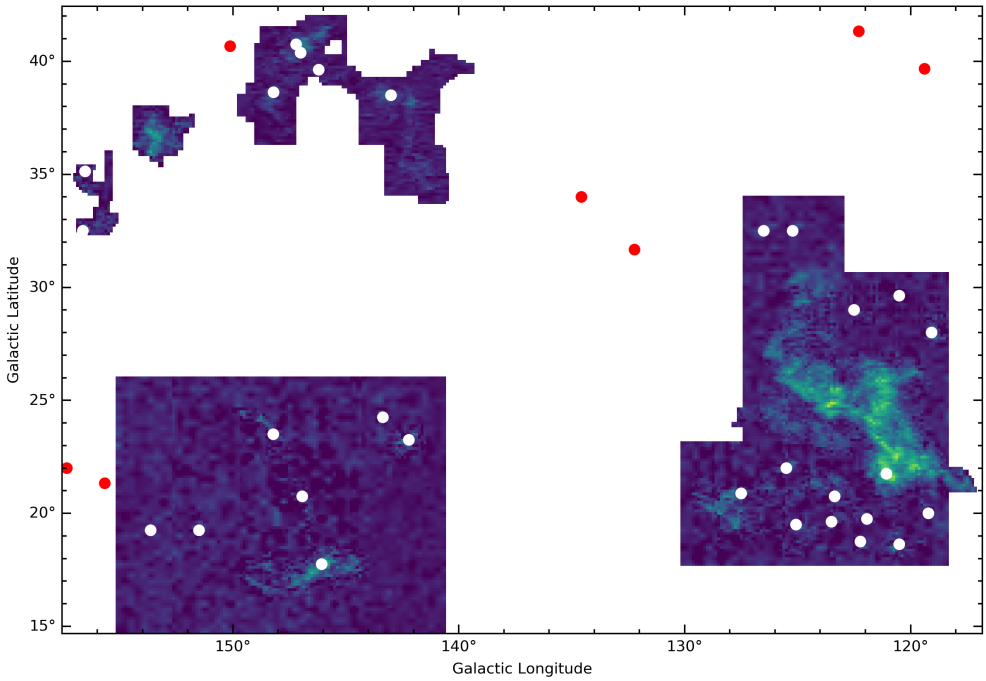

Figure 3. The proposed locations of observations. The red pointings have CO observations, but no detections corresponding to it but were predicted to have molecular material from excess IR from Blitz et al. (1990). The white pointings are the CO centers of clouds identified in Heithausen et al. (1993), and whose molecular mass content and environment could be accurately studied using GBT OH observations and archival CO measurements combined.

the 1665 and the 1667 MHz lines. The 1612 MHz line shows RFI more often and some data will have to be ignored. 1720 MHz emission is generally RFI-free, but time-variable and polarized RFI may be present, which can be easily identified. We opt to have the notch filter in to block out the known strong RF from 1.25 - 1.35 GHz, to prevent any potential faint baseline ripples in the spectra. The RFI table was consulted when choosing which CRRLs to add to this survey, 5 lines that are 20-30 MHz away from known RFI sources were added to the remaining VEGAS IFs.

REFERENCES

Abdo, A., Ackermann, M., Ajello, M., et al. 2010, ApJ, 710, 133

Allen, R. J., Hogg, D. E., & Engelke, P. D. 2015, ApJ, 149, 14

Blitz, L., Bazell, D., & Desert, F. X. 1990, ApJ, 352, L13

Busch, M., Allen, R., Engelke, P., et al. 2019, ApJ, 883

Donate, E., White, J., Magnani, L., et al. 2019, MNRAS, 486, 4414

Fukui, Y., Torii, K., Onishi, T., et al. 2015, ApJ, 798

Glover, S. C. O., & Smith, R. J. 2016, MNRAS, 462, 3011

Grenier, I. A., Casandjian, J.-M., & Terrier, R. 2005, Sci, 307, 1292

Heithausen, A., Stacy, J. G., de Vries, H. W., Mebold, U., & Thaddeus, P. 1993, A&A, 268, 265

Kalberla, P. M. W., Burton, W. B., Hartmann, D., et al. 2005, A&A, 440, 775

Murray, C. E., Peek, J. E. G., Lee, M.-Y., & Stanimirovic, S. 2018, ApJ, 862

Neufeld, D. A., & Wolfire, M. G. 2016, ApJ, 826, 12

—. 2017, ApJ, 845, 15

Pineda, J. L., Langer, W. D., Velusamy, T., & Goldsmith, P. F. 2013, A&A, 554

Planck Collaboration, Ade, P. A. R., Aghanim, N., et al. 2011, A&A, 536

Salas, P., Oonk, J. B., Emig, K. L., et al. 2019, A&A, 626, 16

Seifried, D., Haid, S., Walch, S., Borchert, E. M., & Bisbas, T. G. 2019

Velusamy, T., Langer, W. D., Pineda, J. L., et al. 2010, A&A, 521

Wolfire, M. G., Hollenbach, D., & McKee, C. F. 2010, ApJ, 716

DRAFT VERSION JANUARY 31, 2020
Typeset using LaTeX default style in AASTeX63

The Kinematics and Distribution of Diffuse H_2 in the Outer Galaxy

MICHAEL BUSCH

1. DISSERTATION PLAN

The following document is the general introduction to the use of OH to trace dark molecular gas and how my thesis will eventually be organized. The topics deal with the kinematics and distribution of the dark molecular gas as traced by OH. This document is not a part of the scientific justification.

2. INTRODUCTION TO DARK MOLECULAR GAS

The formation of molecular hydrogen gas, H_2 from atomic hydrogen, H I in galaxies is widely considered to be a critical step for the formation of new stars from the interstellar gas, as molecular lines are an important cooling mechanism to allow star formation in cold and dense molecular clouds. It is thus is one of the most important processes that occurs in the interstellar medium (ISM). Unfortunately, as a symmetric molecule without a dipole moment, H_2 lacks any easily excited rotational states and is practically invisible in emission at the temperature range of 10-100K expected for the bulk of the ISM in the Galaxy, and indirect estimates are required that make use of surrogate tracers. The most universally-accepted surrogate tracer for H_2 in the ISM is the lowest-energy rotational spectral line of ^{12}CO(1-0) at $\lambda = 3$mm. This line is relatively bright and easily observed, often with instrumentation designed specifically for that purpose. CO observations are commonly used jointly with an empirically-derived conversion factor, usually called the "X-factor" (see Bolatto et al. 2013, for a review). The strength of the 3-mm CO line emission is measured in units of K km s^{-1} and, by multiplying this line strength by the X-factor, one directly obtains an estimate of the H_2 column density (particles per unit area).

A growing body of observational evidence points to an extra component of the ISM not traced by either the 21-cm H I line or ^{12}CO(1-0) emission. This excess component is usually referred to as "dark gas" (Grenier et al. 2005; Wolfire et al. 2010). Grenier et al. (2005) showed that the dark gas may be comparable in mass to the CO-bright component, and is widespread. Quantifying how much dark gas exists is therefore of great astronomical interest in an effort to calibrate the "X-factor" and work towards a single prescription for scaling between a molecular tracer line emission and an accurate total molecular mass of H_2. While the 21 cm line is well understood and directly comes from the spin-flip transition of hydrogen atoms, it was the assumption that CO traces all of H_2 which seemed most suspect. Wolfire et al. (2010) developed the model behind the 'dark molecular gas', which explained the missing gas as an issue of low density H_2 not being traced by the CO molecule. The proposed theory being that in environments where there is not enough column density to shield against the ambient interstellar radiation by starlight, the CO molecule will be photodissociated while the H_2 molecule can still exist. Recently, I confirmed in Busch et al. (2019) that the OH molecule is ubiquitous in this density regime and is an effective tracer of diffuse H_2.

The other prevailing theory posits that there is a significant amount of strongly saturated, optically thick (and thus underestimated) H I dominating the 'dark gas'. Recent H I observations with angular resolution comparable to the infrared data have shown that this is not the case, and that the 'dark gas' is most likely H_2 missed by CO observations (Murray et al. 2018). These developments heighten the necessity for a new molecular gas tracer for the diffuse molecular hydrogen.

I propose to use the hydroxyl molecule (OH) as a tool for discovering the distribution and motions of the diffuse molecular hydrogen ($n \sim$ 1-1000 cm^{-3}) in the Galaxy, which has been shown to be dark in CO emission (Wannier et al. 1993; Allen et al. 2012, 2015; Busch et al. 2019). The OH molecule is less abundant and much more faint than CO, but is widely observed with sensitive observations. It does not appear to become fainter in low density environments. While CO all-sky surveys are currently available (e.g. Heyer et al. 1998; Dame et al. 2001), and have for the past few decades led the way in our understanding of the distribution and structure of H_2 in the Galaxy, it has undoubtedly missed a large component of diffuse H_2.

OH as a tracer for H_2provides distinct advantages over CO. The ground-state OH emission lines (1612 MHz, 1665 MHz, 1667 MHz, and 1720 MHz) can be detected, although faint, and can effectively trace this diffuse component of H_2. It is also almost always optically thin, that is, we can garner three-dimensional kinematic information along the line of sight about the diffuse H_2. CO is almost always optically thick and thus a poor tracer of galactic structure and kinematics. With this new tool we propose to answer some interesting questions about the physics and galactic structure of the diffuse molecular gas.

3. PHYSICAL STATE AND STRUCTURE OF DARK GAS IN A ONE-SQUARE-DEGREE

My previous work on this topic focused on a dense survey of OH emission towards a quiescent region of sky in the Outer Galaxy, over a square degree. This 'One-Square-Degree' (OSD) survey was originally designed to probe the structure of the dark gas with OH, and compare directly to the CO. This work followed up a sparse survey by Allen et al. (2015), which showed OH features appearing and disappearing on large spatial scales of 30 parsecs. The OSD looked at much smaller spatial scales at 7 parsecs. We also used another CO survey with higher sensitivity, which allowed a confirmation of the behaviour that CO is dark towards many pointings with detectable OH emission.

I shown in Busch et al. (2019) that volume density is an important consideration in low density galactic environments. This is most likely because the CO molecule's J=1 state is not sufficiently populated by collisional excitation in low density environments for the radiative decay of the J=1-0 to be efficient and bright (set by the molecule's Einstein A_{21} coefficient for spontaneous emission). The density at which collisional de-excitation and spontaneous emission is roughly equal is called the critical density. Far above this threshold density, the emission rate becomes independent of volume density. Thus, for a CO survey at a certain sensitivity, it seems to be the case that CO will be biased towards densities larger or approaching it's critical density, where the J=1 state will be sufficiently populated. For CO, the critical density is $n^* \sim 1000$ cm^{-3}, while for OH $n^* \sim 1$ cm^{-3}and the relevant levels will be collisionally populated in any galactic environment.

4. THESIS PROJECTS

Busch et al. (2019) was a study of the physics of the diffuse ISM using OH. To complete my thesis in the next $\sim$ year and a half, we have identified several interesting problems in Galactic structure, distribution and kinematics of the diffuse molecular hydrogen that OH emission can provide new information on that make use of existing data that have been observed in the past few years but never analyzed:

First, **we wish to remeasure the thickness of molecular gas** in the Perseus Arm using OH. The CO thickness is approximately half that of the atomic gas as traced by H I. The results of the OSD have shown that OH reveals a much more extended portion of H_2, and we expect that it will show a much thicker molecular disk. This would have important implications for our understanding of the spatial and mass distribution of atomic and molecular gas in the ISM.

Secondly, **we want to establish whether or not the molecular gas of the ISM also takes part in the "rolling motions"** of the H I discovered more half a century ago by the Dwingeloo Telescope and discussed by Yuan & Wallace (1973). There is an apparent gradient in radial velocities of the H I. The situation in CO is less clear, and has been deemed "not entirely convincing" by Feitzinger & Spicker (1985).

Finally, **we want to continue to investigate the so-called 'pedestal' feature of OH emission towards the outer galaxy. This is a volume filling molecular gas feature in OH that appears to be co-spatial with atomic gas in H I.** This has never been seen before and such a discovery would be a significant contribution to our understanding of the distribution of the molecular ISM. It might imply a large dark molecular gas mass fraction lying between the spiral arms of our galaxy, hitherto invisible to any other molecular gas tracer.

5. SCALE HEIGHT AND "ROLLING MOTIONS" OF OH EMISSION IN THE OUTER GALAXY

The thickness of the CO emission is, given by a number of surveys, a Gaussian FWHM $\sim$ 90 pc within a R_{gal} = 10 kpc (Heyer & Dame 2015). What is the OH thickness? We expect it to be greater because our assumption is that OH traces the diffuse H_2. With the same data set we can probe the velocity structure of the gas. One open question in galactic structure we can answer is whether or not the OH emission follows the rolling motions as revealed by H I surveys. That is–the gas above the disk appears to have a radial velocity component toward the Sun, and the gas below the disk appears to have a radial velocity component away from the Sun. The theory presented in Yuan & Wallace (1973) posits that the rolling motions are not actually "rolling", but because of the geometry and warp of the Milk Way causes a derivative of velocity with galactic latitude–we suspect so, but CO evidence is inconclusive, most likely due to the clumpy nature of the CO clouds. We should be able to conclusively answer the question about whether or not molecular gas exhibits this behaviour and perhaps comment on preferable warp models. Recent evidence by *Gaia* has shown that the warp of the galaxy causes the observed gradient of velocities in both young and old stars (Poggio et al. 2018). Radio line kinematics from OH would complement the *Gaia* data as the stellar signatures are optical light and susceptible to dust extinction and reddening in the plane of the Galaxy. Does the observed signal also arise in molecular gas? This would reinforce the claim that the warp is a gravitational induced phenomenon. However there are differences between the young and old stars, and the young stars would inherit the kinematics of the gas–using OH to trace these kinematics would provide valuable information to constrain these models.

6. THE NATURE OF THE EXTENDED OH EMISSION IN THE OUTER GALAXY

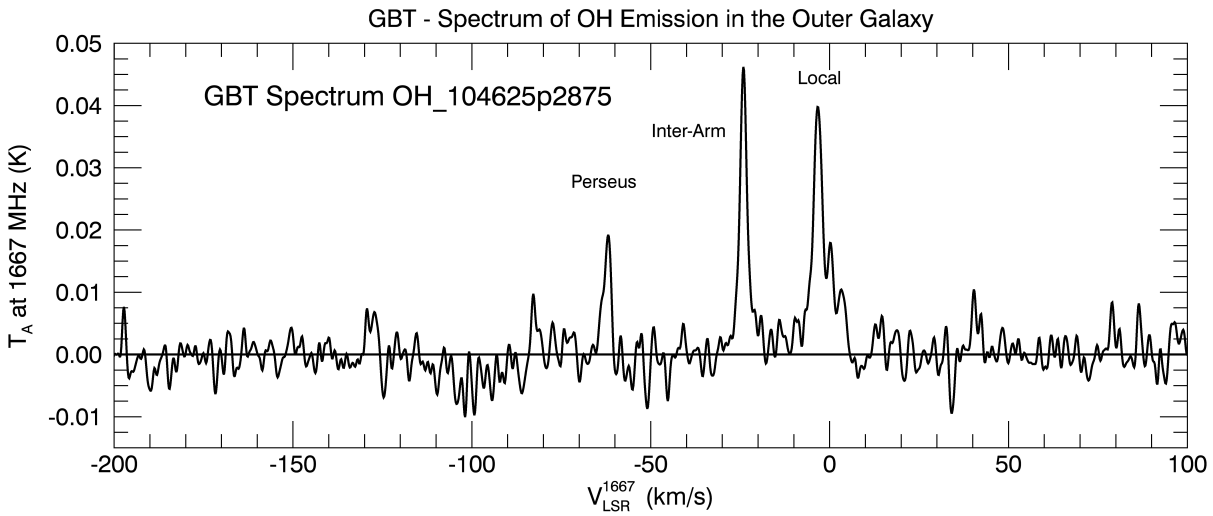

Figure 1. Above: Example of a 1667 MHz OH spectrum from the One Square Degree survey. This spectrum was taken at $l = 104.^{\circ}625, b = +2.^{\circ}875$ with 2 hr of exposure time on the 100m Green Bank Telescope. We consider any feature detected between -75 and -50 km s^{-1} to be associated with the Perseus Arm. In this spectrum, the OH feature associated with Perseus Arm is located near -65 km s^{-1}. Smaller OH features, possibly spurious, can be observed sometimes at -80 km s^{-1} and at -120 km s^{-1}, corresponding to the Outer Arm and Outer Scutum-Crux Arm respectively.

Typical molecular gas tracers (CO, OH, etc) are usually observed as quite narrow emission lines corresponding to spiral arms in the outer galaxy (see Fig. 1). The unusual "pedestal" OH feature (see Fig. 2) was first unexpectedly discovered in spectra recorded with the 100m GBT radio telescope in 2015. This "pedestal" is a faint, wide-band feature which appears to underly the more clumpy emission from molecular clouds along the line of sight through the Galaxy from the sun outwards to the outer reaches of the Galactic disk at low latitudes.

In the summer of 2018, I re-observed the same feature in both 1667 ($T_{mb} \sim 7$ mK) and 1665 ($T_{mb} \sim 4$ mK) MHz OH emission using 100 hours of the 20m dish at the Green Bank Observatory. Observing with a *different telescope* was imperative step in confirming the discovery. Since the structure of the instrumental effects of the 20m telescope is *completely* different than the 100m GBT, this heightened our confidence in the result.

An exploratory program to probe the height (a latitude cut) of this feature and whether or not it is a 'disk' (a longitude cut) was undertaken in the summer of 2019 using 100 hours of GBT Director's Discretionary time. If confirmed, it may imply a rather large diffuse H_2 gas mass co-spatial with the H I and lying between the spiral arms.

The existence of an extended disk of molecular gas in the outer galaxy is clearly a significant new discovery. No one has ever done radio spectroscopy at this sensitivity before. It is imperative to test this hypothesis in as many different ways as possible.

7. CONCLUSION

The 18-cm OH lines, with their low critical density of $n^* \sim 1$ cm^{-3}, are collisionally excited over a large fraction of the quiescent galactic environment and, for observations of sufficient sensitivity, provide an optically-thin radio tracer for diffuse H_2. The results of this proposed work will show that OH emission can contribute significant new perspectives of the structure, distribution and dynamics of molecular hydrogen in the Galactic ISM.

REFERENCES

Allen, R. J., Hogg, D. E., & Engelke, P. D. 2015, ApJ, 149, 14

Allen, R. J., Rodríguez, M. I., Black, J. H., & Booth, R. S. 2012, AJ, 143, 8

Bolatto, A. D., Wolfire, M., & Leroy, A. K. 2013, ARAA, 51, 207

Busch, M. P., Allen, R. J., Engelke, P. D., et al. 2019, ApJ, 883, 158

Dame, T. M., Hartmann, D., & Thaddeus, P. 2001, ApJ, 547, 792

Feitzinger, J. V., & Spicker, J. 1985, MNRAS, 214, 539

Grenier, I. A., Casandjian, J.-M., & Terrier, R. 2005, Sci, 307, 1292

Heyer, M., & Dame, T. M. 2015, Annu. Rev. Astron. Astrophys, 53, 583

Heyer, M. H., Brunt, C., Snell, R. L., et al. 1998, ApJS, 115, 241

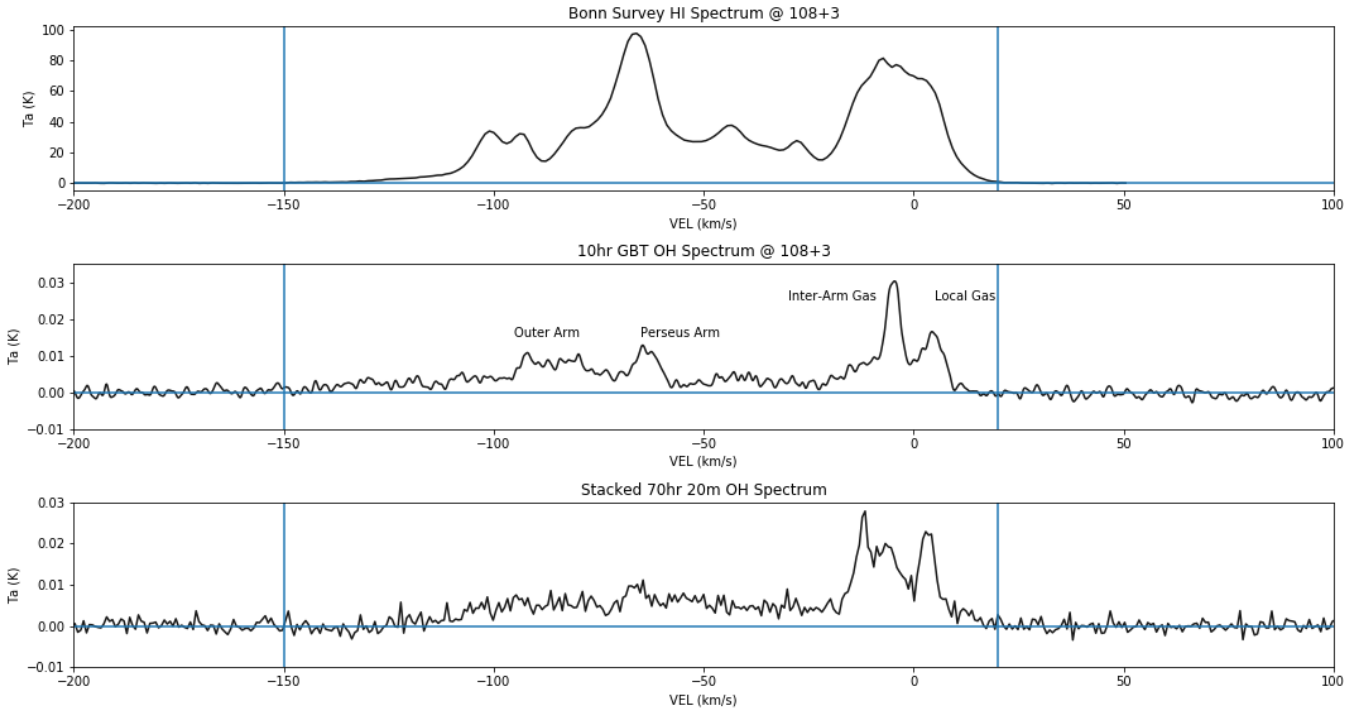

Figure 2. Above: Examination of these spectra shows a broad OH emission feature extending from the lumpy emission of nearby molecular clouds (around zero velocity) out to about -150 km s^{-1}, indicative of a broad ring of differentially-rotating gas extending from the solar neighborhood out to the outer reaches of the H I disk of Galaxy. Superposed on this disk are occasional lumps of OH emission as the line of sight encounters discrete features, for instance the molecular clouds visible near the Perseus spiral arm of the the Galaxy at about -65 km s^{-1}($\approx$ 3.2 kpc from the sun), and in the Outer Arm near -85 km s^{-1}($\approx$ 7.0 kpc from the sun). The appearance of a very similar velocity-extended feature in spectra taken with two very different radio telescopes indicates first: that the "disk" emission comes from a spatially-extended region in the sky covering of order half a degree or more; and second: that it is not likely to arise from poorly-defined instrumental effects. Note that, according to the kinematics of the disk, our location in it, and the particular direction in which the telescope is pointed, no emission is expected at positive radial velocities (and none is seen in H I).

Murray, C. E., Peek, J. E. G., Lee, M.-Y., & Stanimirovic, S. 2018, ApJ, 862

Poggio, E., Drimmel, R., Lattanzi, M. G., et al. 2018, MNRAS, 481, L21

Wannier, P. G., Andersson, B.-G., Federman, S. R., et al. 1993, ApJ, 407, 163

Wolfire, M. G., Hollenbach, D., & McKee, C. F. 2010, ApJ, 716

Yuan, L., & Wallace, C. 1973, ApJ, 185, 453